OXFORD

A guide to facilitate the creation of a femoral tunnel for arthroscopic ligamentum teres reconstruction: a three-dimensional computed tomography study

Abdul Veli Ismailoglu [1,2]*, Pelin Ismailoglu[3], Samir I. Zeynalov[4], Omer Ozdogmus[1],
Saliha Elif Yildizhan[5], Alp Bayramoglu[2] and Asim Kayaalp[6]

[1]Department of Anatomy, School of Medicine, Marmara University, Maltepe Basibuyuk Yolu, No: 9, Maltepe, Istanbul 34854, Turkey, [2]Department of Anatomy, School of Medicine, Acibadem University, Kayisdagi cad., Kerem Aydinlar Kampusu, No: 32, Atasehir, Istanbul 34752, Turkey, [3]Department of Physiotherapy and Rehabilitation, Faculty of Health Sciences, Fenerbahce University, Metropol İstanbul, Ataşehir Blv, Atasehir, Istanbul 34758, Turkey, [4]Department of Orthopaedics & Traumatology, Ardahan State Hospital, Inonu Mah., Sugoze, Ardahan Merkez, Ardahan 75000, Turkey, [5]Department of Biostatistics and Medical Informatics, School of Medicine, Acibadem University, Kayisdagi cad., Kerem Aydinlar Kampusu, No: 32, Atasehir, Istanbul 34752, Turkey and [6]Department of Orthopedic Surgery, Ankara Cankaya Hospital, Barbaros Sk. No: 44, Cankaya, Ankara 06700, Turkey

*Correspondence to: A. V. Ismailoglu. E-mail: abdulveli.ismailoglu@gmail.com

ABSTRACT

The ideal femoral tunnel passing through the centre of the femoral neck targeted to the footprint of the ligamentum teres (LT) is established during the LT reconstruction surgery with the free-hand technique. We aimed to quantitatively determine the entry site and define the angular orientation of the ideal femoral tunnel with its relevance to the femoral valgus angle (FVA) and the femoral anteversion angle (FAA) to facilitate the creation of an ideal femoral tunnel during the LT reconstruction surgery. A total of 60 randomly selected CT images were obtained to reconstruct three-dimensional femur models. A virtual reamer representing the ideal femoral tunnel was placed in the femur models. The femur length, FVA, FAA, the femoral tunnel anterior angle, the femoral tunnel superior angle and the skin- and bony-entry sites were measured. The femoral tunnel angular orientation was strongly correlated with the FVA and the FAA. Mathematical formulas were defined by which entry site of the reamer and the anterior and superior angulation of the femoral tunnel could be estimated before the surgery. The mean skin-entry site was 67.3 mm distal and 0.1 mm anterior to the centre of the greater trochanter's superior border. The angular orientation of the femoral tunnel using FVA and FAA can be easily estimated using mathematical formulas before LT reconstruction surgery. The entry site and angular orientation of the femoral tunnel described in this study can be used to reduce dependency on the usage of fluoroscopy and the workload on the surgeon during the LT reconstruction surgery.

INTRODUCTION

The ligamentum teres (LT) is a conical structure that contains the anterior branch of the posterior division of the obturator artery but poorly contributes to the stabilization of the hip between the femoral head and acetabular fossa [1]. However, recent studies have indicated an association between articular damage and LT injuries [2], suggesting the importance of LT for the stabilization of the hip joint. In addition, the stabilization role of LT may become necessary in the deficiency of normal bony architecture, such as in the case of dysplastic hips [3].

An injured LT may occur with adduction-flexion and axial loading, excessive rotation or twisting [4]. Since LT houses nociceptors [5, 6] and mechanoreceptors [7], injured LT can act as a potential pain generator. Debridement of the LT tears

with radiofrequency ablation has demonstrated outstanding outcomes to overcome hip pain in most individuals [8, 9]. However, in some cases, the pain persisted, and, in that situation, LT reconstruction surgery has been indicated to reinstate hip joint stability and increase the associated function. Therefore, studies recommend the LT reconstruction surgery in such cases [10–13]. Since patient-reported early outcomes are favourable [14, 15] and numerous studies have already described the detailed surgical technique of the LT reconstruction [11, 16–18], it is reasonable to expect the LT reconstruction surgery may become more frequent procedure than before.

During the LT reconstruction surgery, the femoral tunnel must be created after the graft preparation to insert the graft on the fovea capitis. Before reaming the femoral tunnel, a guide
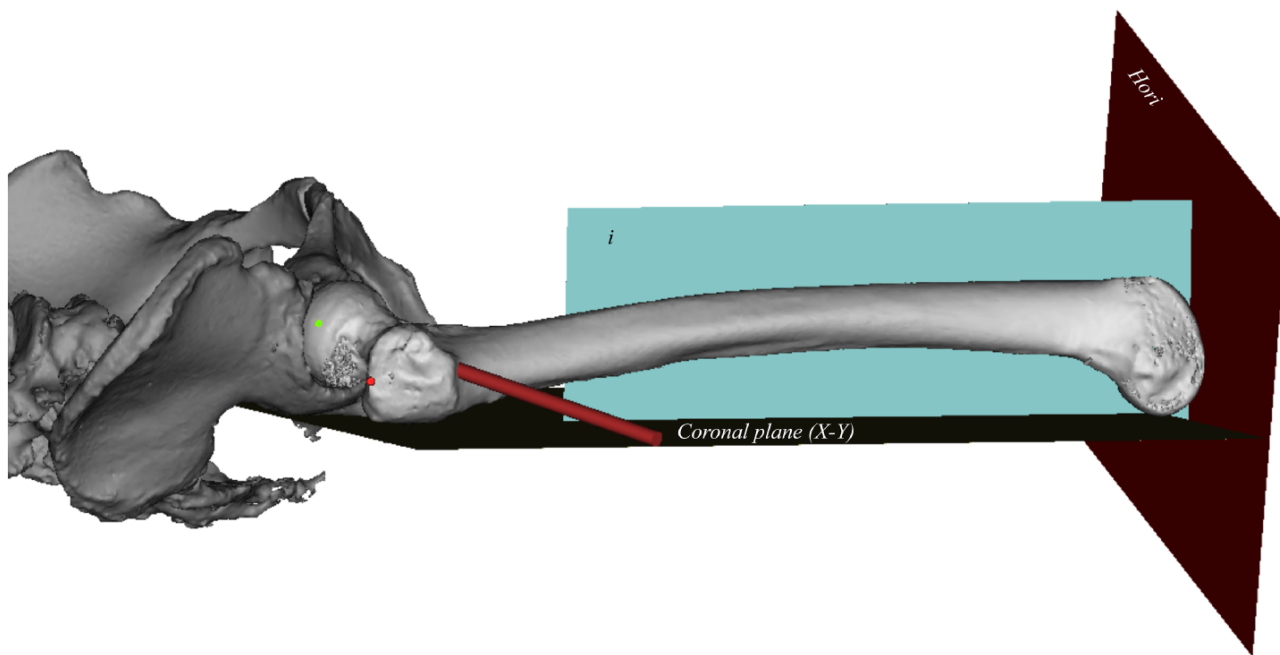
Fig. 1. Lateral view of the right femur with customized anatomical coordinate planes. The green point, LT footprint-fovea capitis; the red point, centre of the greater trochanter's superior border (CGT); red rod, neck-centred and LT footprint-targeted virtual reamer.

pin is introduced, starting from the lateral cortex of the greater trochanter and exiting through the footprint of LT. Furthermore, the guide pin should run through the femoral neck centre to achieve an ideal femoral tunnel and avoid femoral neck fractures during the reaming of the tunnel. This approach is adopted in a 'free-hand' technique under fluoroscopic guidance [19, 20]. However, precisely anticipating the entry site and angulation of the guide pin in advance is believed to facilitate a surgeon's determination of the femoral tunnel entry site and orientation during the LT reconstruction surgery. In this way, the time spent by the surgeon in adjusting the angular orientation of the femoral tunnel and the amount of fluoroscopy radiation exposure to the patient during this procedure can be significantly reduced, which also reduces the surgery cost.

In this study, our main aim was to quantitatively determine the entry site and define the angular orientation of the ideal femoral tunnel to facilitate the LT reconstruction surgery. Furthermore, we measured the femoral valgus angle (FVA) and the femoral anteversion angle (FAA) to investigate their correlations with the femoral tunnel angulation and the entry site of the tunnel. For these purposes, we placed a virtual reamer representing the femoral tunnel in the 3D femur model to define the femoral tunnel angular orientation. We accordingly hypothesized that both the skin- and bony-entry sites of the reamer change depending on FVA and FAA.

MATERIALS AND METHODS

This study was designed as a retrospective study in order to acquire enough number of CT images. Since the all personal data of patients were legally confidential, all scans were fully anonymized by the hospital radiology service staffs. We were only able to access the CT images and not any identifiable information of the participants was included in the manuscript. The

study protocol was approved by the Institutional Review Board of the authors.

In this retrospective study, lower extremity CT scans obtained between October 2015 and August 2021 from 65 randomly selected patients were examined along with their clinical records. The CT scans were obtained with the Somatom Force device (Siemens Healthineers Global, Germany) using standard techniques at 100 kVp and 256 mAs, with a slice thickness of 0.5–1.0 mm and a resolution of 512×512 pixels (voxels approximately $0.7 \times 0.7 \times 0.5$ mm^3).

Five patients, who presented with femur fracture and severe femoral osteoarthritis, were excluded from the study. The measurements were performed using 60 CT scans (41 male and 19 female) of mean age 49.1 ± 13.6 years (age range: 20–76 years).

The Digital Imaging and Communications in Medicine format data of each CT scan were imported to Mimics software (version 21.0, Materialize, Leuven, Belgium) to reconstruct a 3D geometric femur model. The scans included the entire lower extremity along with the lumbar vertebrae and pelvis. The femur model was reconstructed using a threshold mask (range: 226 HU to 3071 HU) according to the guidelines of the software. The pelvic bones were also reconstructed to provide hints regarding the position of the femur (Fig. 1). All measurements were performed on the 3D femur models.

The femoral tunnel, which extended between the lateral cortex of the femur and the LT footprint, should be created during the LT reconstruction surgery using a 7-mm or 8-mm reamer. Therefore, to identically imitate the reamer used in the surgery, a virtual 7-mm-diameter, 150-mm-long model of a generic reamer was constructed using a commercially available 3D modelling program (RHINOCEROS 3D; McNeel) and imported into the Mimics as a standard tessellation language (STL) file. The virtual
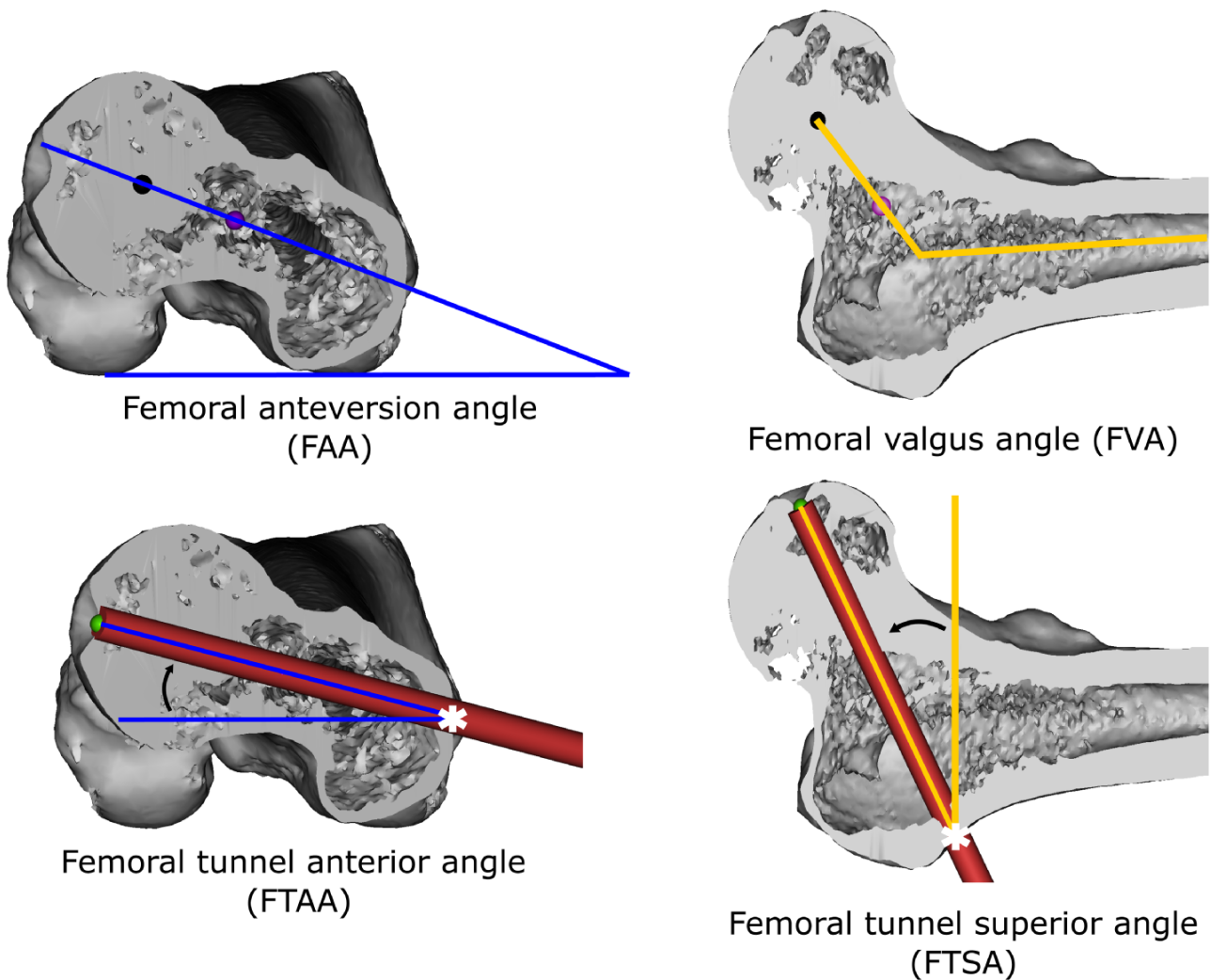
Fig. 2. The measurements of the FAA, FVA, FTAA and FTSA on the 3D femur model. Left and right upper panel images showing the femoral neck axis. Black arrows depict the magnitude of FTAA and FTSA. *The bony-entry site of the reamer.

reamer model passing through the centre of the femoral neck was placed in the 3D femur model with its medial end on the LT footprint-fovea capitis.

Establishing the femur-customized anatomical coordinate system was critical to ensure the validity of the measurements. Hence, after the reconstruction of the geometric femur model, an idealized coordinate system was reconstructed using specific femur bony landmarks to standardize the femur orientation. Three planes perpendicular to each other, representing the global Cartesian X–Y, X–Z and Y–Z planes, were created as described by Su *et al.* (Fig. 1) [21].

The reconstructed 3D femur model was imported into the 3-Matic software (version 13.0, Materialise N.V., Belgium) as an STL file to conclude the centre of the femoral head and the neck more precisely as well as to avoid observer error using the least-squares approach and the centre of gravity equation, respectively [22]. Then, the femoral neck axis (FNA) was defined as a line passing through the centre of the femoral head and the centre of the femoral neck.

MEASUREMENTS

Following the construction of the femur-customized anatomical coordinate system, the femur length was measured. The FAA and the FVA were measured using the FNA determined by the algorithms described earlier (Fig. 2). FAA was defined as an angle between the FNA and the line passing through the most prominent posterior points of the femoral condyles. The angle between the FNA and the line passing through the centre of the proximal femoral medullary canal was defined as FVA. The virtual 3D reamer was placed passing through the femoral neck centre, beginning from the LT footprint and its entrance on the femur lateral cortex (bony-entry site) was marked with an * sign. The angle formed between the axis of the virtual reamer and the transverse line starting from the bony-entry site was defined as the femoral tunnel anterior angle (FTAA). In the coronal section of the femur model, the femoral tunnel superior angle (FTSA) was also defined as an angle formed between the axis of the virtual reamer and the vertical axis that began from the bony-entry site and extended medially (Fig. 2). FTAA in the
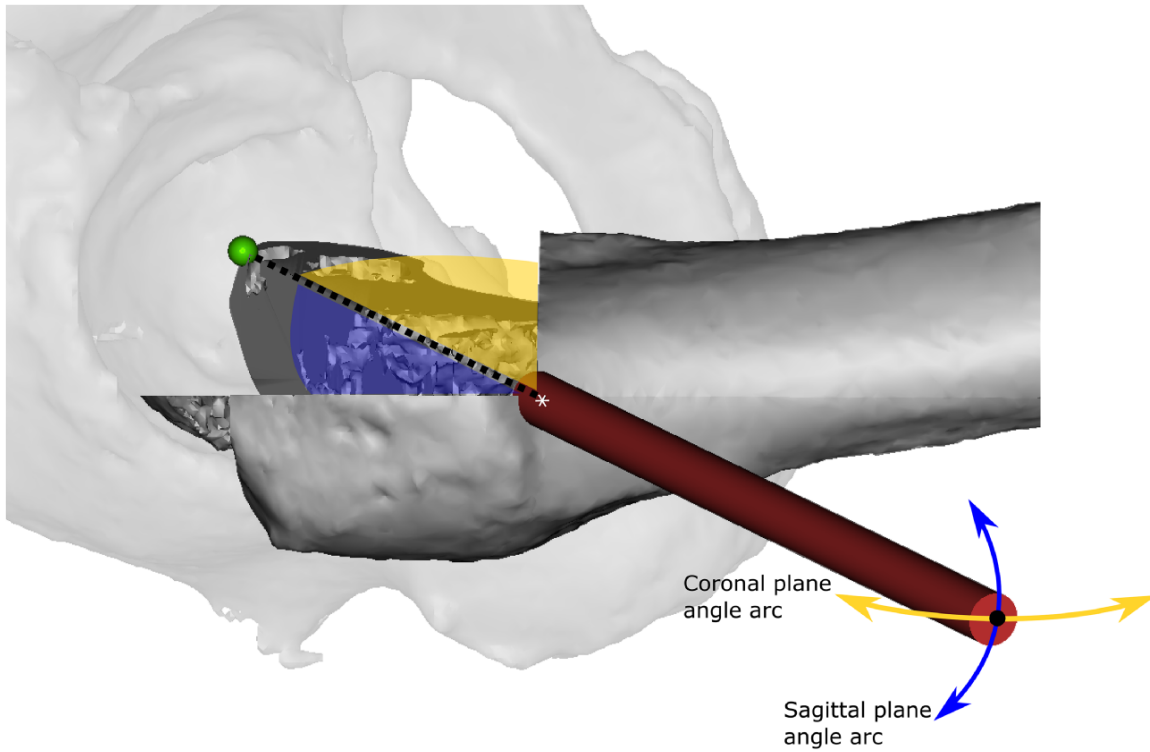
Fig. 3. Lateral view of the right femur with an inserted virtual reamer. Blue and yellow regions indicate anteroposterior and superior-inferior angulation of the femoral tunnel, respectively. The black dotted line, ideal angular orientation of the femoral tunnel; green point, LT footprint.
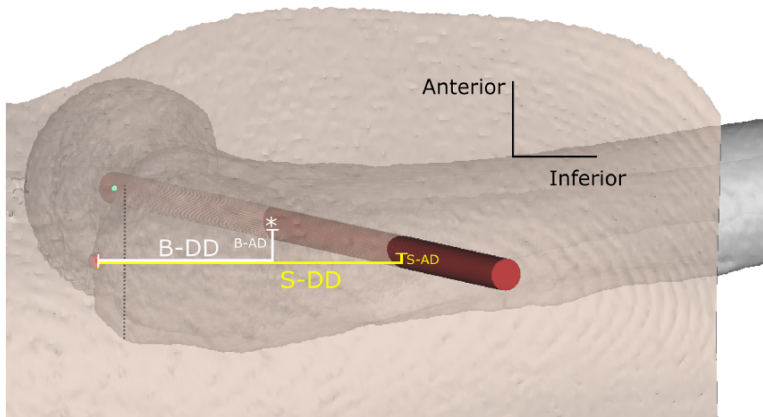

Fig. 4. Lateral view of the 3D femur model with overlying transparentized skin. Bony-distal distance (B-DD), bony-anterior distance (B-AD), skin-distal distance (S-DD) and skin-anterior distance (S-AD) were measured to determine the bony and the skin-insertion sites of the reamer.

sagittal plane and FTSA in the coronal plane, defining the angular orientation of the femoral tunnel, are two essential required angles that should be determined to create the neck-centred and LT footprint-targeted femoral tunnel during the LT reconstruction surgery (Fig. 3). The Pearson's correlation test and linear regression analysis were also applied to determine the extent of change of FTAA and FTSA depending on FAA and FVA, respectively.

The virtual skin of the femoral region was constructed (as per the suggestion of the Mimics software, range: −718 HU to −177 HU), followed by partial transparentizing of the constructed skin to view the underlying femur model. After aligning the virtual reamer to represent ideal femoral tunnel orientation, the entry site of the reamer was defined both on the virtual femoral skin and the femoral bone using the greater trochanter's superior border (CGT) (Fig. 4).

Table I. *Measured angles and distances to identify the orientation of the neck-centred and LT footprint-targeted femoral tunnel*

		Mean	SD	Minimum	Maximum
Femoral valgus angle (FVA)		123.7^0	4.9^0	114.4^0	137.2^0
Femoral anteversion angle (FAA)		11.5^0	8.7^0	−7.2^0	38.1^0
Femoral tunnel superior angle (FTSA)		25.6^0	5^0	17^0	43^0
Femoral tunnel anterior angle (FTAA)		6.8^0	8.7^0	−10.7^0	35.2^0
Skin-entry site	Skin-distal distance	67.3 mm	13.2 mm	40.4 mm	117 mm
	Skin-anterior distance	0.1 mm	12.5 mm	−48.2 mm	25.8 mm
Bony-entry site	Bony-distal distance	42 mm	4.1 mm	30 mm	53.1 mm
	Bony-anterior distance	7 mm	3.6 mm	−1.1 mm	16.8 mm

Distances were measured according to the CGT.
mm, milimeters.

Table II. *Pearson's correlation tests*

Array 1—independent variables	Array 2—dependent variables	Significance	r Value
FVA	FTSA	P < 0.001	0.83
FAA	FTAA	P < 0.001	0.92
FAA	Skin-anterior distance	P < 0.001	−0.83
FAA	Bone-anterior distance	P < 0.001	−0.70
FVA	Skin-distal distance	P < 0.001	0.52
FVA	Bone-distal distance	P = 0.026	0.28

FVA femoral valgus angle, FAA femoral anteversion angle, FTSA femoral tunnel superior angle, FTAA femoral tunnel anterior angle.

Table III. *Linear regression equations*

Mathematical formulas to estimate the dependent variables

FTSA = −86.989 + 0.911 × FVA
FTAA = −3.731 + 0.919 × FAA
Skin-anterior distance = 13.919–1.195 × FAA
Bone-anterior distance = 10.333–0.286 × FAA

FVA femoral valgus angle, FAA femoral anteversion angle, FTSA femoral tunnel superior angle, FTAA femoral tunnel anterior angle.

bony-distal distance were not strong ($r < 0.70$). Therefore, linear regression equations were not calculated for the distal distances (Table III).

STATISTICAL ANALYSES

SPSS software (SPSS Inc., Chicago, IL) was applied for statistical analyses. The variables were investigated through virtual and analytical methods to determine whether they were normally distributed. Descriptive statistics were presented as mean ± standard deviation. The calculation of Pearson's product-moment correlation coefficients (r) between arrays of dependent and independent variables was analysed. Once the correlation analysis was complete, a linear regression analysis was applied for only high-degree correlated variables ($r > 0.70$). $P < 0.05$ was considered to indicate statistical significance.

RESULTS

The femur length mean was 443.8 ± 34.8 mm (min 363.1 mm, max 532.5 mm). Measured angles and measured entry site distances are shown in Table I. When the femur was retroverted, the FAA was noted as a minus. Similarly, posteriorly positioned FTAA and posteriorly located distances were noted as minus (see Table I, FTAA, minimum and Table II). The mean superior and the mean anterior angulations of the femoral tunnel (FTSA and FTAA) were 25.6^0 and 6.8^0, consecutively. The mean skin-anterior distance was 0.1 mm and the mean bony-anterior distance was 7 mm according to the CGT.

All correlations tested in this study were significant (Table II). However, *r* values between FVA and skin-distal distance, and

DISCUSSION

In this study, the angular orientation of the femoral tunnel and its entry site were investigated by inserting a virtual reamer into a 3D femur model. Our study confirms that the superior and anterior angulation of the femoral tunnel was strongly correlated with the FVA and the FAA, respectively. The mean skin-entry site of the reamer was located 67.3 mm distal and 0.1 mm anterior to the CGT. A surgeon can easily estimate the skin incision site and the angulation of the reamer by considering the results of this study to create a femoral tunnel during the LT reconstruction surgery.

In LT reconstruction surgery, the guidewire is placed to select the femoral tunnel line. The guidewire should be placed in a retrograde fashion, starting from laterally over the greater trochanter through the femoral neck to exit the LT footprint-fovea capitis for the ideal location of the femoral tunnel [11, 23]. Past studies have suggested that the femoral neck should be drilled through its centre [10, 24] as it may be important to avoid potential femoral neck fractures after the surgery. Targeting the LT footprint for the creation of the femoral tunnel is also necessary to avoid cartilage damage of the femoral head as well as to reconstruct the anatomical nature of LT. Therefore, fluoroscopy is frequently applied to create neck-centred and LT footprint-targeted ideal femoral tunnel. We placed a 7-mm virtual reamer representing the ideal femoral tunnel on the 3D femur model. The ideal femoral tunnel's mean superior angle (FTSA) and the mean anterior angle (FTAA) were 25.6^0 and 6.8^0, respectively. We believe that placing the guidewire initially

at these angles facilitates the establishment of the femoral tunnel line and reduces the workload of the surgeon by minimizing the dependency on the usage of fluoroscopy during surgery. In patients with extreme femoral valgus or anteversion deformities, by pre-operatively calculating the femoral tunnel alignment and its entrance by using the formulas supplied in this study, the surgeon can practically estimate and place the initial guidewire in a correct alignment, and then can proceed to create the definite femoral tunnel.

Since FVA and FAA were strongly correlated with the angular orientation of the femoral tunnel, we applied mathematical formulas using linear regression analysis (Table III) such that a surgeon could pre-operatively determine the patient-specific angular orientation of the femoral tunnel, which can be useful, especially in patients with excessive femoral valgus and femoral anteversion deformities. For example, the anteversion angle of the femur models in this study spanned between -7.2^0 and 38.1^0, which indicates that some of the femur models were retroverted (minus degrees of FAA) (Table I). In this case, posterior angulation of the femoral tunnel (minus degrees of FTAA) is required to target the LT footprint, and the magnitude of the posterior or anterior angulation can be estimated using the formula presented in this study.

To the best of our knowledge, only one study has so far quantitatively described the bony-entry site of the femoral tunnel. Using nine digitized femurs, Brady et al. reported that the mean femoral tunnel entry site was located 7.0 mm distal and 5.8 mm anterior, according to the centre of the vastus ridge on the femur [16]. However, detecting the centre of the vastus ridge over the skin during the surgery can be unlikely, making it difficult to locate the incision site. Therefore, we defined the entry site of the femoral tunnel over the skin according to CGT that can be easily used as a landmark during the surgery. The mean femoral neck centred skin insertion site was located 67.3 mm distal and 0.1 mm anterior according to CGT. Both anterior and distal distances were correlated with the FAA and FVA, respectively (Table II). However, only the anterior distance was strongly correlated and could be estimated using a mathematical formula before the surgery (Table III). This correlation was found to be negative, which indicates that, as the FAA increases, the reamer should be positioned further posterior to the CGT to acquire an ideal femoral tunnel position.

We also measured the bony-entry site of the femoral neck centred reamer located 42 mm distal and 7 mm anterior to the CGT. Only in one case, the bony-entry site was detected posterior to the CGT and noted as a minus. Therefore, a surgeon can consider that the bony entrance of the reamer is generally located anterior to the CGT. However, an anterior distance of the skin-entry site spanned anterior and posterior to the CGT, depending on the anteversion angle of the femur. As the skin was farther from the fovea capitis than the lateral cortex of the femur, due to the presence of the subcutaneous fat, the slightest change in the anteversion angle could change the anterior distance of the skin-entry site to a greater extent relative to the bony-anterior distance, which explains why the skin-anterior distance's correlation coefficient (r-value) was higher than the bony-anterior distance (Table II). The distal distances of both the skin- and bony-entry sites were significantly but moderately correlated with FVA, indicating that the distal distance can partially change depending on FVA. Because of this moderate correlation between distal distances and FVA ($r < 0.70$), a linear regression equation was not included in the present study.

Past studies have demonstrated that the LT diameter varies at 6–9 mm [25, 26]. The recommended reamer diameter should be 1 mm larger than the graft to ease the graft passage [10], and the ideal reamer diameter is 7–8 mm. Therefore, the diameter of the virtual reamer used in this study was selected as 7 mm. It is reasonable to consider that the angulation or the entry site of the femoral tunnel would not change with the diameter size of the reamer.

A surgeon can estimate the angular orientation of the femoral tunnel using the formulas described in this study. Furthermore, a surgeon can determine both the skin- and bony-entry sites of the reamer using CGT as a landmark. We thus believe that these formulas and descriptions of the entry sites can facilitate the creation of a neck-centred and LT footprint-targeted ideal femoral tunnel with less usage of fluoroscopy, which, in turn, can reduce the time and cost of the LT reconstruction surgery.

We recognize that this study has some limitations as it was conducted on the 3D femur models. The femur customized coordinate system was created similar to that specified in other studies to standardize the measurements. However, the position of the femur may differ in the surgery; thus, the angles to be applied in the surgery may not exactly match those in this study. However, our study suggested a strong correlation among FVA, FAA and femoral tunnel angulation and described formulas that can be useful to anticipate the angular orientation of the femoral tunnel before surgery. Moreover, the thickness of the fat tissue between the skin and the femur was not measured in this study, which may affect interpretation related to the skin-distal and skin-anterior distances.

CONCLUSION

The most important finding of this study is that the superior and anterior angulations of the femoral tunnel were strongly correlated with the FVA and the FAA, which, in turn, can be used to estimate the patient-specific femoral tunnel angulation pre-operatively using formulas supplied in this study to facilitate the creation of the femoral tunnel during LT surgery.

DATA AVAIILABILITY

The data underlying this article will be shared on reasonable request to the corresponding author.

ACKNOWLEDGEMENTS

None declared.

FUNDING

The authors declare that no funds, grants or other support were received during the preparation of this manuscript.

CONFLICT OF INTEREST STATEMENT

The authors have no relevant financial or non-financial interests to disclose.

AUTHORS' CONTRIBUTIONS

Conceptualization: AV Ismailoglu; Methodology—collecting clinical and radiographic data: O Ozdogmus and SI Zeynalov; Methodology—analysis of radiographic data: AV Ismailoglu, P Ismailoglu and SE Yildizhan; Writing—original draft preparation: AV Ismailoglu; Writing—review and editing: A Bayramoglu, Asim Kayaalp.

ETHICAL APPROVAL

This study was conducted retrospectively from data obtained for clinical purposes in line with the principles of the Declaration of Helsinki. The study protocol was approved by the IRB of the authors and Acibadem University Research Ethics Board (No. 2021-10/10).

REFERENCES

1. Kapandji I K. The physiology of the ligamentum teres. *Physiol Jt* 2011; **2**: 24–5.
2. Kaya M, Suziki T, Minowa T *et al.* Ligamentum teres injury is associated with the articular damage pattern in patients with femoroacetabular impingement. *Arthroscopy* 2014; **30**: 1582–7.
3. Martin RL, Palmer I, Martin HD. Ligamentum teres: a functional description and potential clinical relevance. *Knee Surg Sports Traumatol Arthrosc* 2012; **20**: 1209–14.
4. Rao J, Zhou YX, Villar RN. Injury to the ligamentum teres - mechanism, findings, and results of treatment. *Clin Sport Med* 2001; **20**: 791–9.
5. Leunig M, Beck M, Stauffer E *et al.* Free nerve endings in the ligamentum capitis femoris. *Acta Orthop Scand* 2000; **71**: 452–4.
6. Sarban S, Baba F, Kocabey Y *et al.* Free nerve endings and morphological features of the ligamentum capitis femoris in developmental dysplasia of the hip. *J Pediatr Orthop B* 2007; **16**: 351–6.
7. Wenger D, Miyanji F, Mahar A *et al.* The mechanical properties of the ligamentum teres - a pilot study to assess its potential for improving stability in children's hip surgery. *J Pediatr Orthop* 2007; **27**: 408–10.
8. Byrd JWT, Jones KS. Traumatic rupture of the ligamentum teres as a source of hip pain. *Arthroscopy* 2004; **20**: 385–91.
9. Haviv B, O'Donnell J. Arthroscopic debridement of the isolated ligamentum teres rupture. *Knee Surg Sports Traumatol Arthrosc* 2011; **19**: 1510–3.
10. O'Donnell J, Klaber I, Takla A. Ligamentum teres reconstruction: indications, technique and minimum 1-year results in nine patients. *J Hip Preserv Surg* 2020; **7**: 140–6.
11. Philippon MJ, Pennock A, Gaskill TR. Arthroscopic reconstruction of the ligamentum teres: technique and early outcomes. *J Bone Joint Surg Br* 2012; **94**: 1494–8.
12. Rosinsky PJ, Annin S, Maldonado DR *et al.* Arthroscopic ligamentum teres reconstruction: minimum 2-year patient-reported outcomes with subanalysis of patients with ehlers-danlos syndrome. *Arthroscopy* 2020; **36**: 2170–82.
13. Matthewson G, Williams A, Macciacchera M *et al.* Effective management options for treatment of microinstability of the hip: a scoping review. *Curr Rev Musculoskelet Med* 2023; **16**: 9–18.
14. Knapik DM, Farivar D, Kunze KN *et al.* Indications and outcomes after ligamentum teres reconstruction: a systematic review. *Arthrosc Sports Med Rehabil* 2021; **3**: e939–e49.
15. Shapira J, Yelton MJ, Rosinsky PJ *et al.* Ligamentum teres reconstruction may lead to improvement in outcomes following a secondary hip arthroscopy for symptomatic microinstability: a systematic review. *Arthroscopy* 2021; **37**: 1811–9.e1.
16. Brady AW, Chahla J, Locks R *et al.* Arthroscopic reconstruction of the ligamentum teres: a guide to safe tunnel placement. *Arthroscopy* 2018; **34**: 144–51.
17. Simpson JM, Field RE, Villar RN. Arthroscopic reconstruction of the ligamentum teres. *Arthroscopy* 2011; **27**: 436–41.
18. Lindner D, Gilat R, Domb BG. Ligamentum teres injuries and treatment. In: Bonin N, Randelli F, Khanduja V (eds), *Hip Preservation Surgery: Open, Arthroscopic, and Endoscopic Techniques*. Berlin, Heidelberg: Springer, 2020, 181–90.
19. Lindner D, Sharp KG, Trenga AP *et al.* Arthroscopic ligamentum teres reconstruction. *Arthrosc Tech* 2012; **2**: e21–e5.
20. Chandrasekaran S, Martin TJ, Close MR *et al.* Arthroscopic reconstruction of the ligamentum teres: a case series in four patients with connective tissue disorders and generalized ligamentous laxity. *J Hip Preserv Surg* 2016; **3**: 358–67.
21. Su XY, Zhao JX, Zhao Z *et al.* Three-dimensional analysis of the characteristics of the femoral canal isthmus: an anatomical study. *Biomed Res Int* 2015; **2015**: 459612.
22. Zhang R-Y, Su X-Y, Zhao J-X *et al.* Three-dimensional morphological analysis of the femoral neck torsion angle—an anatomical study. *J Orthop Surg Res* 2020; **15**: 192.
23. Mei-Dan O, McConkey MO. A novel technique for ligamentum teres reconstruction with "all-suture" anchors in the medial acetabular wall. *Arthrosc Tech* 2014; **3**: e217–e21.
24. Menge TJ, Mitchell JJ, Briggs KK *et al.* Anatomic arthroscopic ligamentum teres reconstruction for hip instability. *Arthrosc Tech* 2016; **5**: e737–e42.
25. Lorda-Diez CI, Canga-Villegas A, Cerezal L *et al.* Comparative transcriptional analysis of three human ligaments with distinct biomechanical properties. *J Anat* 2013; **223**: 593–602.
26. Philippon MJ, Rasmussen MT, Turnbull TL *et al.* Structural properties of the native ligamentum teres. *Orthop J Sports Med* 2014; **2**: 2325967114561962.26.